THE RETARDING POTENTIAL ANALYZER FOR DYNAMICS EXPLORER-B

W. B. HANSON, R. A. HEELIS, R. A. POWER, C. R. LIPPINCOTT,
D. R. ZUCCARO, B. J. HOLT, L. H. HARMON and S. SANATANI
Center for Space Sciences, The University of Texas at Dallas, Richardson, TX 75080, U.S.A.

(Received 11 May, 1981)

Abstract. The Retarding Potential Analyzer for Dynamics Explorer B measures the bulk ion velocity in the direction of the spacecraft motion, the constituent ion concentrations and the ion temperature along the satellite path. These parameters are derived from a least squares fit to the ion number flux versus energy curve obtained by sweeping or stepping the voltage applied to the internal retarding grids of the RPA. In addition, the spectral characteristics of irregularities in the total ion concentration are determined by high time resolution measurements and by use of a comb filter. These data are obtained from a separate wide aperture sensor.

1. Introduction

The planar retarding potential analyzer (RPA) is a device that measures the energy spectrum of the ambient thermal ions in the vehicle frame of reference on the Dynamics Explorer-B (DE-B) spacecraft. The instrument described here has a lineage that goes back over 20 y [1, 2, 3]. Its predecessors have been flown on several rockets, Air Force satellites, OGO-6, Viking, and Atmosphere Explorers (AE) C, D, and E. Initially the RPA was used to measure the ion concentration (N_i) and ion temperature (T_i). In satellites it can also sort N_i into its constituent parts if the various ions present have widely different masses. On OGO-6 a sensitive mode for studying detailed changes in N_i was introduced [2] that was intended to look for whistler 'ducts'. Even here these functions are ascribed to the 'duct' mode, though the techniques employed have evolved considerably. Tests with the OGO-6 data also revealed the capability of measuring the bulk ion velocity component normal to the sensor face, and this parameter was routinely derived from the AE data. On AE both the ion characteristic curves and their derivatives were measured since it was anticipated that the latter would be more easily analyzed [3]. On Viking, digital stepping of the retarding potential was employed, rather than a continuous voltage ramp [4].

In conjunction with the Ion Drift Meter (IDM), also described in this volume [5], the complete bulk ion velocity vector $\mathbf{V}_d$ is measured from DE-B. This quantity is fundamental to many of the science objectives of DE at all latitudes. The ion motion affects the ion temperature, both enhancing [6] and diminishing [7] it, and it can also strongly perturb the ion composition at high latitudes [8]. In addition, it has been observed on AE that there is often a strong correlation between $\mathbf{V}_d$ and N_i down to scale sizes of less than 1 km. Various kinds of plasma instabilities are suspected to be operative in the ionosphere, but to date good evidence for them, particularly at high and mid latitudes,

Space Science Instrumentation 5 (1981) 503–510. 0377–7936/81/0054–0503 $01.20.

has not been well documented. The combined $\mathbf{V}_d$ and N_i data from DE will cover a large dynamic range in both amplitude and scale size, and it is reasonable to expect that a significant amount will be learned about plasma turbulence, the more so because of the electric and magnetic wave fields also being measured.

2. Instrument Description

2.1. RPA Sensor functions

The DE RPA utilizes the planar retarding potential analyzer sensor shown in Figure 1, which is oriented with its front face nearly normal to the vehicle velocity vector. Ions entering the aperture in the sensor face pass through a region that is electrically segmented by a series of gold plated tungsten grids before striking the solid collector. The collector ion currents are measured by a linear, automatic ranging electrometer.

The two sensor entrance grids are grounded to the vehicle and surrounded by a conducting ground plane. The next grid inward is the double retarding grid, to which a time-varying electric potential is applied. The suppressor grid is held at a negative potential (≈ -15 V) to prevent low-energy ambient electrons from reaching the collector and to prevent secondary-electron escape from the collector. The function of the shield grid is to protect the electrometer connected to the collector from the electrical transients generated by changing potentials on the retarding grids; it is also held at vehicle ground. All the grids are woven from 0.025 mm (1 mil) wire, and the number of wires per inch for each grid (in two perpendicular directions) is indicated in parentheses in the figure.

The retarding potential is variable in the range from approximately $+32$ to 0 V. The details of this voltage trace, and whether it is continuous or stepped, depend on the operating mode of the instrument. The automatic ranging absolute linear electrometer measures the collector current versus retarding voltage, and the derivative of the ion current with respect to retarding voltage can also be measured simultaneously.

The derivative is measured by superposing a small 3400-Hz voltage on the retarding grid voltage. The modulation of the ion current with respect to the retarding grid voltage, is synchronously detected, then amplified and filtered before being presented to the spacecraft data acquisition system. The main electrometer has 8 sensitivity ranges, with adjacent ranges differing in sensitivity by $10^{1/2}$, whereas the ranging derivative amplifier has six sensitivity ranges (also with $10^{1/2}$ sensitivity ratio). During the derivative operation the main electrometer and the derivative amplifier can each be monitored by 2 minor frame analog telemetry words, or all 4 words can be assigned to the derivative amplifier. The sensitivity ranges of the two devices are both monitored with minor frame digital words.

The ion-current characteristics measured in these modes is the primary data transmitted to the ground from the RPA. Subsequently a least-squares fitting technique is used to retrieve the ion temperature, total ion (electron) concentration, information on the composition of major ions, the vehicle potential, and the component of the ion-drift velocity that is parallel to the sensor normal (v_d). In essence this velocity component is

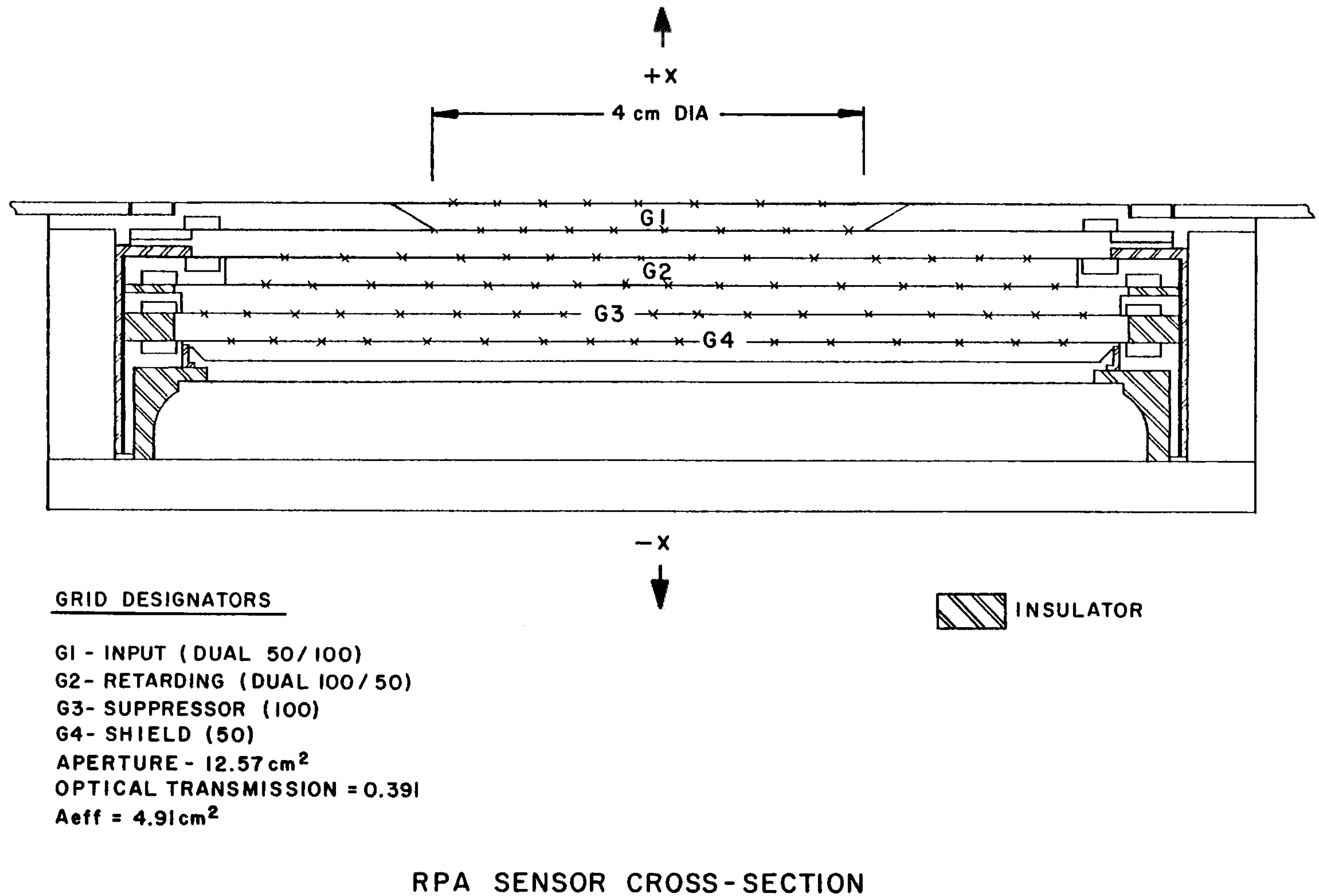

Fig. 1. Schematic cross section of RPA sensor. All exposed surfaces and inner elements of the RPA sensor, except insulators, are gold plated. The numbers in parenthesis describing the grids give the number of one mil wires per inch. The nominal grid element separation is 2.5 mm.

extracted from the least-squares fitting by finding the mean energy separation between ions of different mass and comparing this energy to that expected from just the vehicle velocity itself.

2.2. Duct sensor functions

On previous missions we have utilized the same sensor on a time-share basis to measure both the RPA curves and the small scale irregularities in N_i. A separate sensor is used here for the N_i measurements to avoid time sharing and to achieve a faster electrometer response by using a larger collecting area. The duct sensor is shown in Figure 2. It has approximately 5 times greater effective collecting area than the RPA sensor, and except for the negative electron-suppressor grid all elements are held at spacecraft ground.

The ion current to the collector is measured 64 times per second, approximately every 120 m of flight path. These measurements can be taken directly from the duct electrometer, or from a difference amplifier that examines changes in the ion current with a 10 times increase in sensitivity. To prevent aliasing, these signals are passed through a three-pole Bessel filter with a 32 Hz cutoff before being telemetered.

The ionospheric irregularity measurements are extended to much smaller scale sizes on DE with the aid of a comb filter bank. Six filters are employed, each having a bandwidth of a factor of e (2.72); their frequency ranges and mean scale sizes are given in Table I. These filters are connected to a linear wide band amplifier with 5 sensitivity ranges that differ successively by $10^{1/2}$ in gain. The amplifier sensitivity is controlled by feedback from the filter with the largest output voltage. The filters measure the mean irregularity power within their respective bandwidths with about a 45 ms averaging time.

TABLE I

Comb filter bank characteristics

Filter number	1	2	3	4	5	6
Frequency band (Hz)	32–86	86–233	233–630	630–1700	1700–4600	4600–12 400
Mean scale size (m)	125	46.5	17.2	6.35	2.35	0.87

Their outputs are sampled every 2 s within a period of 375 ms. The wide band amplifier normally monitors the output of the duct electrometer, but every other 2 s period it can be assigned to the difference amplifier output from the Ion Drift Meter [5]. In effect this permits the determination of the irregularity power in the transverse ion drift velocity components at the same scale sizes as those at which N_i irregularities are being examined.

3. Operations

3.1. RPA modes

The various RPA modes are differentiated by the manner in which the retarding potential varies with time. This potential can be varied in continuous linear ramps or it can be

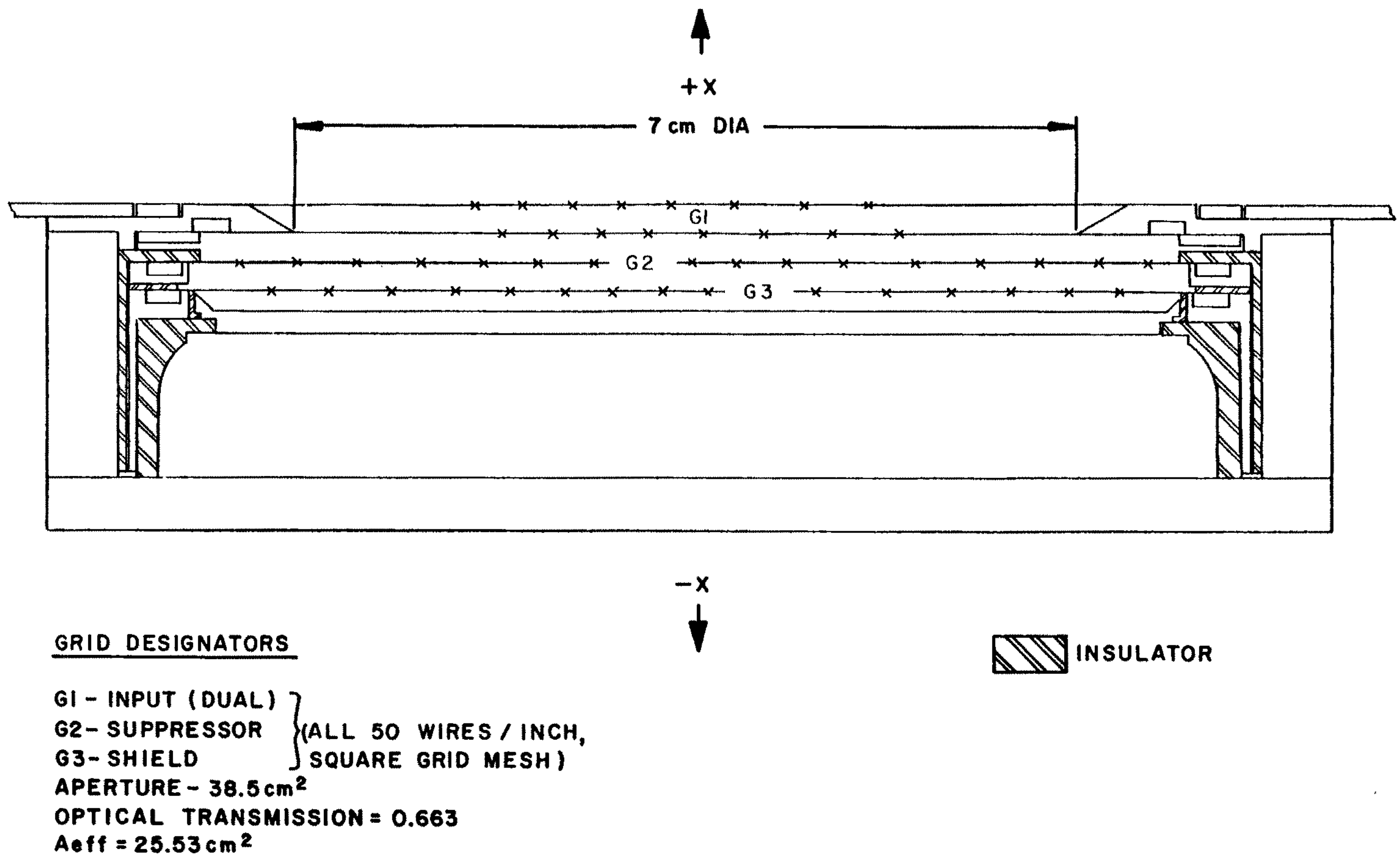

Fig. 2. Schematic cross section of duct sensor. The duct sensor has the same characteristics as the RPA sensor except for the aperture size and the number of grids.

stepped digitally. In both cases a 3400 Hz 'wiggle' voltage of selectable amplitude (including zero) is superposed to permit measurement of the derivative of the thermal ion energy spectrum.

Consider first the stepped digital modes. The digital voltages are obtained from an 8 bit digital-to-analog converter with 10 bit accuracy. The maximum potential of 31.875 V is divided into 255 equal increments (256 positions) of 125 mV each, and the dwell time per step can be either 16 ms or 32 ms. There is also a digital memory with 256 locations made up of 8 blocks of 32 twelve bit words. The first 8 bits of each word define one of 256 voltage stepper positions and the next three bits define the wiggle amplitude to be superposed. The 8 possible wiggle peak to peak amplitudes are 0, 25, 50, 100, 200, 300, 450, and 600 mV. The twelfth memory word bit selects the output of either the main electrometer or derivative amplifier to be telemetered. This memory can be reloaded in an arbitrary manner by ground command. When the memory is used to control the retarding grid potential any two of the 8 blocks can be selected to be used alternately. These 64 steps will occur in one second if 16 ms steps are used, or 2 s if 32 ms steps are selected. It is anticipated that this will constitute the principal RPA mode of operation.

Another mode of digital operation, called the counter mode, has a nearly fixed format with a four-second cycle time. First the ramp voltage is stepped from 31.5 V to zero in 64 0.5 V steps with a finite wiggle amplitude. During the next sweep cycle the ramp voltage is stepped from 7.875 V to zero in 64 0.125 V steps, again with finite wiggle amplitude. These two ramps are normally repeated with zero wiggle amplitude. If a 32 ms dwell time is selected, then only the first two ramps occur, but both the electrometer and derivative amplifier will be sampled each step. The 5 basic linear ramp voltage sweeps available to control the retarding grid potential are described in Table II. All but the first one may be used alone, or the first can be alternated with any of the last four. In addition, the two 12 V or the two 24 V ramps can be alternated. The wiggle amplitude can be separately chosen for sweep No. 1 and its alternate.

TABLE II

RPA linear sweep modes

Sweep No.	1	2	3	4	5
Sweep range (V)	$0 \to 3$	$12 \to 0$	$0 \to 12$	$24 \to 0$	$0 \to 24$
Sweep period (ms)	300	350	350	700	700

3.2. Duct modes

The sampling of changes in the duct sensor ion current is designed to provide higher sensitivity when the ionosphere is smooth than when it is rough. When the ionosphere is rough it is also desirable to have relatively long continuous blocks of data for spectral analysis. This increased sensitivity is achieved in essence by periodically storing the electrometer output voltage at one terminal of a difference amplifier with a gain of 10, then connecting the live electrometer to the other difference amplifier terminal. The difference amplifier output is simultaneously set to the midpoint of the 0–5 V analog output so that both positive and negative changes in N_i can be measured. When $|\Delta N_i/N_i|$ becomes of the order of 0.1 (depending on the electrometer voltage) the difference amplifier will hit either the upper or lower edge of the output band, at which point the duct electrometer is monitored directly. Enable pulses accompanying each of the RPA words on the subcommutated telemetry frame are used to control the timing of this switching procedure. These enable pulses occur every 2 s. If the difference amplifier over-range occurs within 1 s, the words are switched back to the electrometer through the next 8 digital subcom enable pulses (17 to 18 s). At the end of this period, they are switched back to the amplifier. If over-range occurs again within 1 s, the words are switched back to the electrometer for another 17 to 18 s period. If over-range does not occur during the 1 s period, one of the two following events will occur:

(a) An amplifier over-range will switch the words to the electrometer and the next digital subcom enable pulse will initiate a new cycle;

(b) After a 16 s period, the words are switched to the electrometer for 1 minor telemetry frame (6.25 ms) and then a new cycle is initiated. Thus if the ionosphere is relatively smooth, i.e., with $\Delta N_i/N_i$ of less than a few percent, it will be seen in large blocks of amplifier data. If the ionosphere is rough, then large blocks of duct electrometer data will be taken. At high latitudes the ionosphere is almost always rough by these standards.

As previously described, there is a comb filter bank that samples the irregularity power in $(\Delta N_i/N_i)$ every two seconds (every four seconds if the filter is being shared with IDM). It will be possible on command to monitor the first 5 filters every 1/4 s.

4. Data Analysis and Presentation

It is anticipated that all routine data processing will be performed by programs run on the DE Science Data Processing System at Goddard Space Flight Center. Such large quantities of data can be surveyed most effectively by examining visual data displays, and the data will be plotted on microfiche in several different formats to aid in its digestion. Many of the data, particularly derived parameters, will also be stored on the computer in mission analysis files (MAF's) [9]. For checking data validity and for examining small scale phenomena, routine plots will be made of measured ion characteristic curves and their computer fits, as well as of the raw data and spectral analysis of 4 s (and larger) segments of the duct detector data.

Plots of ionospheric parameters will usually be made in 20 min frames. A routine merging of the ram ion drift velocity component from the RPA with the transverse components from the Ion Drift Meter will take place using data from the mission analysis files. The combined results will be available on the 20 min time plots as well as in a polar plot format (see IDM description in [5]). The ion temperature, ion constituent concentrations (of H^+, He^+, O^+, and of molecular ions near perigee), the spacecraft potential, the ram ion drift component, and a crude ionospheric roughness parameter will all be plotted together in a 20 min time frame. In addition, the spectral power of ionospheric irregularities over a range of e^{13} in scale size (from less than 1 m to >100 km) will also be plotted in 13 separate spectral bands in 20 min time frames.

Many specialized plot routines, having some flexibility in parameters plotted (including those available from the MAF files from other instruments) as well as in format, will be utilized on graphics terminals. This software will be available to other DE investigators with compatible hardware.

Acknowledgments

We thank E. R. Schmerling and D. P. Caufman for their tireless efforts to make the Dynamics Explorer project a reality, and M. Wiskerchen for aiding in the improvement of the computer facilities available. We also thank J. P. McClure for his assistance with the instrument design and L. A. Swaim and W. E. Lane for the excellent support they have provided in the construction of the instrument. This work was supported by NASA under contracts NAS5-24298, NAS5-26071, NAS5-24297, and NAS5-26068.

References

1. Hanson, W. B. and McKibbin, D. D.: *J. Geophys. Res.* **66**, 1667 (1961).
2. Hanson, W. B., Sanatani, S., Zuccaro, D. R., and Flowerday, T. W.: *J. Geophys. Res.* **75**, 5483 (1970).
3. Hanson, W. B., Zuccaro, D. R., Lippincott, C. R., and Sanatani, S.: *Radio Sci.* **8**, 333 (1973).
4. Hanson, W. B., Sanatani, S., and Zuccaro, D. R.: *J. Geophys. Res.* **83**, 4351 (1977).
5. Heelis, R. A., Hanson, W. B., Lippincott, C. R., Zuccaro, D. R., Harmon, L. H., Holt, B. J., Doherty, J. E., and Power, R. A.: *Space Sci. Instr.* **5**, 511 (1981) (this issue).
6. Schunk, R. W., Raitt, W. J., and Banks, P. M.: *J. Geophys. Res.* **80**, 3121 (1975).
7. Hanson, W. B., Nagy, A. F., and Moffett, R. J.: *J. Geophys. Res.* **78**, 751 (1973).
8. Schunk, R. W., Banks, P. M., and Raitt, W. J.: *J. Geophys. Res.* **81**, 3271 (1976).
9. Smith, Paul H., Freeman, Clyde H., and Hoffman, R. A.: *Space Sci. Instr.* **5**, 561 (1981) (this issue).